Beraunite group minerals and related phosphates

JAROMÍR TVRDÝ

*Department of Geology, Faculty of Science, Masaryk University, Kotlářská 267/2, 611 37 Brno, Czech Republic;
e-mail: jt.geologie@gmail.com*

Abstract

Basic iron phosphates are a complicated group of minerals, despite their relatively simple chemical composition. In a comprehensive work based on the author's doctoral thesis, the individual mineral phases close to beraunite including ferroberaunite, zincoberaunite and tvrdýite are characterized. Genetic conditions of formation and the influence of geological environment on the chemical composition were outlined. The work is completed by characteristic data of structurally related phosphate minerals containing the so-called *h*-cluster, i.e. members of the dufrénite and rockbridgeite groups, of the gormanite-souzalite series, lipscombite and barbosalite.

Introduction

Despite their relatively simple chemical composition, basic iron phosphates are a very complicated group of minerals („perplexing substances in the mineral kingdom", Moore 1969). This includes natural phases related to beraunite, a mineral bearing the name of the Central Bohemian town of Beroun (its German form, respectively; Breithaupt 1840, 1841).

The type locality of beraunite is the long-abandoned Hrbek mine in the municipality of Zaječov. Hrbek was one of a number of small mines supplying the surrounding ironworks with limonite and hematite ores. The main mineralogical discoveries date back to the period of the greatest mining boom in the middle of the 19th century, when the maximum annual production of the mine was close to 1.5 thousand tonnes of ore. On the cracks of the limonite ore, beraunite occurred alone or in the association with other phosphates: cacoxenite (a new mineral from Hrbek described even earlier; Steinmann 1826), dufrénite, strengite, wavellite and delvauxite (Velebil et al. 2018). The distorted name of the locality is also given to *herbeckite*, a half-forgotten, obsolete name for pisolitic ferruginous quartz (Dufrénoy 1847).

A number of localities with the beraunite-related minerals are now known from the Czech Republic. They have been found at other Ordovician iron ore occurrences between Beroun and Rokycany, as supergene phases of phosphate accumulations in granites and pegmatites, and in metamorphosed iron ores and quartzites.

Crystal structure

The crystal structure of beraunite was first solved by Fanfani, Zanazzi (1967) on the basis of single crystal data obtained by the Weissenberg method. The characteristic arrangement of coordination octahedra in basic Fe-phosphates was pointed out by Moore (1965, 1969). A typical structural unit is the so-called *h*-cluster, which occurs in minerals of the beraunite, dufrénite and rockbridgeite groups, and also in the lipscombite-barbosalite series

(Moore 1970; Fig. 1). The basic building block here is a trimer of face shared metal centered octahedra. In "ferrosoferric phosphates" with Fe dominance in all structural sites, the valence of iron in the central octahedron determines the colour of the mineral, ranging from greenish-black for Fe^{2+} - Fe^{3+} to orange, tan and yellow hues for the "oxidised" Fe^{3+} - Fe^{3+} compositions (Moore, Kampf 1992).

The structure of beraunite solved by Moore, Kampf (1992) agrees with the results of Fanfani, Zanazzi (1967). In the structure, the coordinating Fe-octahedra and P-tetrahedra form relatively dense layers oriented parallel to 100, which explains the perfect cleavage along this plane. The structural framework formed by the coordination octahedra contains large open channels oriented along with the stretching axis of the needle-like crystals [010], and these channels contain non-ligand water molecules. Water molecules are connected to each other and to the
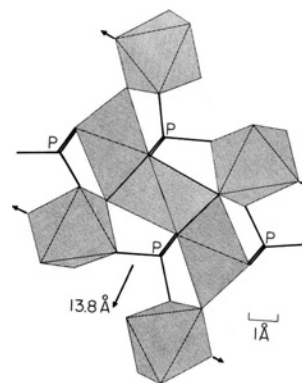

Fig. 1 *The h-cluster and its immediate polyhedral neighbourhood in the basic iron phosphates. The $(PO_4)^{3-}$ tetrahedra, shown as P-O spokes, share corners with the octahedra and are above and below the cluster. Original image of Moore (1970); with permission of the Mineralogical Society of America.*

Fe-polyhedra framework by hydrogen bridges (Fig. 2).

The general formula of beraunite-related minerals is given as $M1M2M3_2M4_2(PO_4)_4(OH,O)(OH)_4(H_2O)_4 \cdot 2H_2O$. The $M1$ site should ideally be preferentially occupied by the "larger" divalent cations (Fe^{2+}, Mn^{2+} and Zn), and the $M2$ to $M4$ sites by the "smaller" trivalent cations (Fe^{3+} and Al; Table 1). However, it appears that this is not always the case, as evidenced in particular by beraunite itself where $M1$ is occupied by Fe^{3+}. Occupation of all octahedral M-sites by trivalent iron causes lowering of the symmetry of the crystal structure and a change in the H-bonding system that transfers electro-valence charges (Vrtiška et al. 2022). In addition, the presence of Al^{3+} at the $M1$ site was observed in the zincoberaunite specimen from Krásno (Tvrdý et al. 2020).

The existence of four independent octahedral sites gives the hypothetical possibility of a large number of mineral phases, but their definition will be very difficult due to the need for detailed structural analysis. The occupation of octahedral sites in minerals related to beraunite is shown in Fig. 3, where hypothetical *manganoberaunite* and *zincotvrdýite* are included for illustration. The combination of individual cations for the phases shown in this figure is given in Table 2.

Influence of local environment on the chemistry of beraunite-related minerals

Hydrated basic phosphates are generally formed from low-temperature water solutions in the supergene and late hydrothermal stages of mineral associations. The composition of the parent solutions is influenced by the rock environment at the site of their origin and formation. The physical and chemical conditions at the place of crystallization of the mineral phases from the solution also play an important role. In principle, two main environments of occurrence of beraunite-related minerals can be distinguished.

In sedimentary and metamorphic rocks, the most common original source of phosphorus is organic material, and consequently mainly apatite formed during diagenesis and metamorphism. Supergene phosphates occur on fractures of host rocks, which are most commonly iron and manganese (meta)sedimentary ores as well as graphitic quartzites. In beraunite-related minerals, only iron, manganese and less frequently aluminium are usually represented in the cationic positions. Alkalis are most commonly bound in the accompanying dufrénite and cacoxenite. Occurrences of this type are known throughout the world. The iron-ore deposits in Hesse and Thuringia (Germany), Gravel Hill Mine (England), Svappavaara (Sweden), Blaton (Belgium), Shady and Three Oaks Gap (Arkansas, USA), and in the Czech Republic belong to the best known localities (see *e.g.* Vrtiška 2023 for details). An interesting site is Mullica Hill (New Jersey, USA), where phosphates occur as concretions and replacements of fossils (belemnites, oysters) in Cretaceous glauconitic sandstone.

In magmatites, especially of granitic composition, and their metasomatic and hydrothermal derivatives, the main source of phosphorus is accumulation of primary phosphates (mainly triphylite in pegmatites and triplite + apatite in hydrothermal-pneumatolytic systems), usually accompanied by chemically varied mineral assemblage, including ore minerals. During alteration of the primary phosphates, metasomatic replacement occurs first, followed by gradual decomposition and leaching. The re-
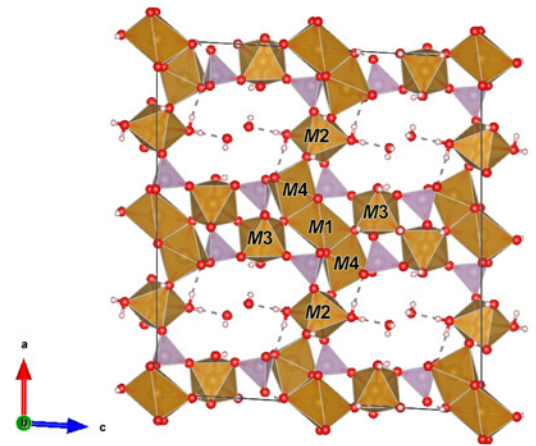

Fig. 2 *Crystal structure of beraunite: coordination octahedra FeO_6 brown, coordination tetrahedra PO_4 grey, O red, H white (data projection after Moore and Kampf 1992).*

Table 1 *Ionic radii of selected cations in in six-fold coordination (Shannon 1976)*

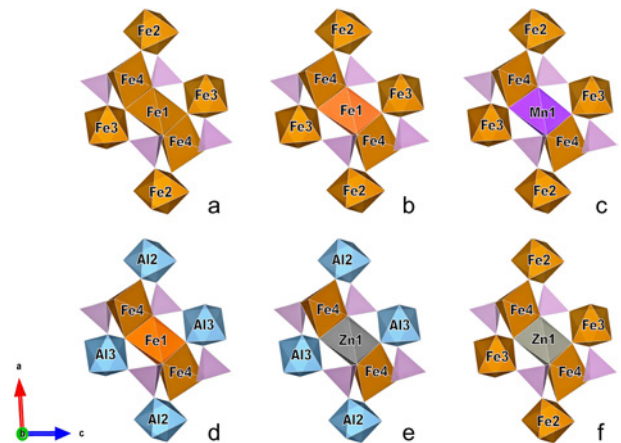| Cation	Ionic radius (Å)
Zn^{2+}	0.740
Mn^{2+}	0.830
Fe^{2+}	0.780
Mn^{3+}	0.645
Fe^{3+}	0.645
Al^{3+}	0.535

Fig. 3 *Occupation of octahedral sites in existing and some hypothetical mineral phases of the beraunite group (M2 octahedra belong to two adjacent units): a) beraunite, b) ferroberaunite, c) hypothetical manganoberaunite, d) tvrdýite, e) hypothetical zincotvrdýite, f) zincoberaunite.*

Table 2 *Occupation of octahedral sites in the existing and some hypothetical mineral phases of the beraunite group as shown in Fig. 3*

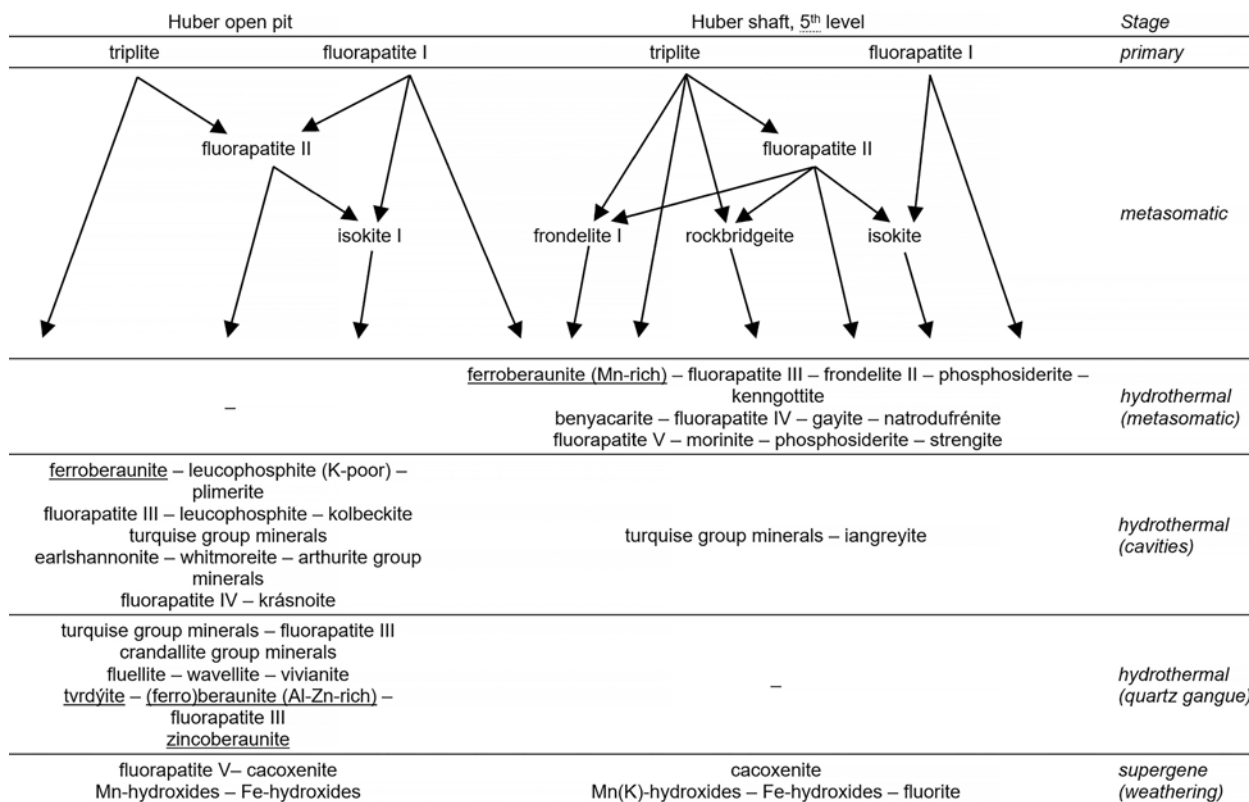| Mineral phase	$M1$	$M2$	$M3$	$M4$
Beraunite	Fe^{3+}	Fe^{3+}	$2Fe^{3+}$	$2Fe^{3+}$
Ferroberaunite	Fe^{2+}	Fe^{3+}	$2Fe^{3+}$	$2Fe^{3+}$
Manganoberaunite (hypothetical)	Mn^{2+}	Fe^{3+}	$2Fe^{3+}$	$2Fe^{3+}$
Tvrdýite	Fe^{2+}	Al^{3+}	$2Al^{3+}$	$2Fe^{3+}$
Zincotvrdýite (hypothetical)	Zn^{2+}	Al^{3+}	$2Al^{3+}$	$2Fe^{3+}$
Zincoberaunite	Zn^{2+}	Fe^{3+}	$2Fe^{3+}$	$2Fe^{3+}$

Fig. 4 *Evolution of phosphate mineral associations observed at the Huber open pit (left) and the 5th level of the Huber shaft (right), Krásno, Czech Republic; underlined are beraunite related minerals (Sejkora et al. 2006, modified).*
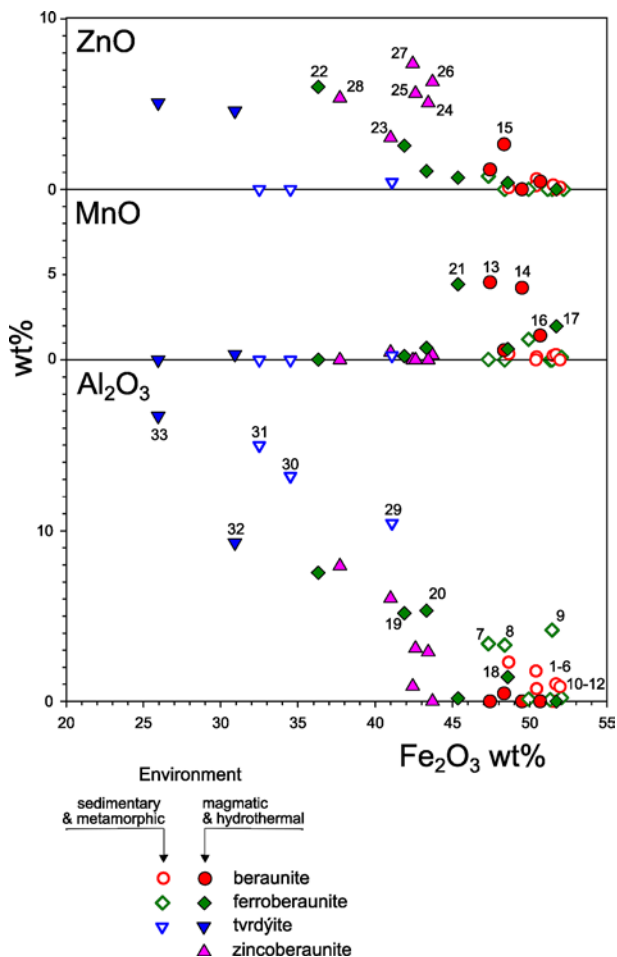
sulting secondary mineral associations tend to be very diverse (Fig. 4); in the case of the beraunite-related phases, zinc and aluminium are mainly present in addition to iron and partly manganese. Among the world localities, the best known are pegmatites in the USA (Foote, North Carolina; Palermo, New Hampshire), Brazil (Sapucaia, Minas Gerais), Bavaria (Hagendorf, Zwiesel-Hühnerkobel), and phosphate occurrences in Portugal (Bendada, Folgosinho, etc.).

The chemical composition of beraunite and related minerals from the two geological environments described above can be seen from the diagram in Fig. 5. The points of specimens from sedimentary and metamorphic rock environments are indicated by blank symbols and those from pegmatites and pneumatolytic rocks by solid symbols. The bottom Fe_2O_3/Al_2O_3 plot shows generally higher Fe contents in the samples of the first group, which often come from iron-ore deposits. Conversely, zinc and manganese contents are relatively higher in the second type of environment. A small group of manganese-rich beraunite and ferroberaunite stand out in the Fe_2O_3/MnO plot; none of the samples could show Mn dominance in the $M1$ site. The Fe_2O_3/ZnO plot delineates a group of points with elevated zinc content. The Al-Zn-rich ferroberaunite from Krásno (*Al-rich beraunite*; Sejkora et al. 2016) fits very well into the zincoberaunite field, but Zn dominance in the $M1$ site was not found there.

Fig. 5 *Diagram of the relation of Al_2O_3, MnO and ZnO contents to Fe_2O_3 in beraunite-related minerals. For more details see the text, for point numbering see Table 3.*

Table 3 *Overview of the samples plotted in Fig. 5*

No.	Mineral	Locality	Environment	Reference
1	Beraunite	Poniklá	Fe-Mn ores	new data
2	Beraunite	Ullersreuth	Fe-Mn ores	new data
3	Beraunite	Waldgirmes	Fe-Mn ores	new data
4	Beraunite („eleonorite")	Waldgirmes	Fe-Mn ores	Chukanov et al. (2017)
5	Beraunite (original specimen)	Hrbek	Fe-Mn ores	Vrtiška et al. (2022)
6	Beraunite (neotype)	Hrbek	Fe-Mn ores	Vrtiška et al. (2022)
7	Ferroberaunite	Černovice	quartzite	Vrtiška et al. (2017)
8	Ferroberaunite	Svappavaara	Fe-Mn ores	new data
9	Ferroberaunite	Svappavaara	Fe-Mn ores	Chukanov et al. (2016)
10	Ferroberaunite	Blaton	quartzite	new data
11	Ferroberaunite (type)	Gravel Hill	Fe-Mn ores	Tvrdý et al. (2022)
12	Ferroberaunite (Mn-rich)	Morašice	Fe-Mn ores	Vrtiška et al. (2019a)
13	Beraunite (Mn-rich)	Hagendorf South	pegmatite	Aksenov et al. (2018)
14	Beraunite (Mn-rich)	Mangualde	pegmatite	Marzoni Fecia di Cossato et al. (1989)
15	Beraunite	Hagendorf South	pegmatite	new data
16	Beraunite	Hagendorf South	pegmatite	new data
17	Ferroberaunite	Lutomia, Poland	pegmatite	Włodek et al. (2015)
18	Ferroberaunite	Hagendorf South	pegmatite	new data
19	Ferroberaunite	Krásno	pneumatolyte	new data
20	Ferroberaunite (Al-rich)	Hagendorf South	pegmatite	new data
21	Ferroberaunite (Mn-rich)	Krásno	pneumatolyte	Sejkora et al. (2006)
22	Ferroberaunite (Al-Zn rich)	Krásno	pneumatolyte	Sejkora et al. (2016)
23	Zincoberaunite-tvrdýite?	Hagendorf South	pegmatite	new data
24	Ferroberaunite (Zn-rich)	Hagendorf South	pegmatite	new data
25	Beraunite (Zn-rich)	Hagendorf South	pegmatite	new data
26	Zincoberaunite (cotype)	Hagendorf South	pegmatite	Chukanov et al. (2016)
27	Zincoberaunite (type)	Hagendorf South	pegmatite	Chukanov et al. (2016)
28	Zincoberaunite	Krásno	pneumatolyte	Tvrdý et al. (2020)
29	Tvrdýite-Fe^{3+} (?)	Waldgirmes	Fe-Mn ores	new data
30	Tvrdýite	Krušná Hora	Fe-Mn ores	Vrtiška et al. (2019b)
31	Tvrdýite	Krušná Hora	Fe-Mn ores	Vrtiška, Malíková (2020)
32	Tvrdýite-ferroberaunite	Hagendorf South	pegmatite	Aksenov et al. (2018)
33	Tvrdýite (type)	Krásno	pneumatolyte	Sejkora et al. (2016)

Minerals of the beraunite group

The beraunite group is referred to here, although it is not approved by the Commission on New Minerals, Nomenclature and Classification of the International Mineralogical Association (*e.g.* mindat.org or Aksenov et al. 2018). Currently, the group comprises four valid members (Table 4). A classification diagram for the existing beraunite-related minerals with Fe^{3+} dominance at the *M*2-*M*4 sites is shown in Fig. 6.

Beraunite

Beraunite is the only member of the group with trivalent iron dominance in the central *M*1 site. From the publication of Frondel (1949) until the new redefinition of beraunite (Tvrdý et al. 2021; Vrtiška et al. 2022), this mineral

Table 4 *Comparative data for minerals of the beraunite group*

Mineral	Symbol	Space group	*a* (Å)	*b* (Å)	*c* (Å)	β (°)	*V* (Å³)	Ref.*
Beraunite $Fe^{3+}_6(PO_4)_4O(OH)_4 \cdot 6H_2O$	Bru	*Cc*	20.651	5.138	19.215	93.523	2034.8	(1)
Ferroberaunite $Fe^{2+}Fe^{3+}_5(PO_4)_4(OH)_5 \cdot 6H_2O$	Fbru	*C2/c*	20.871	5.159	19.226	93.319	2066.7	(2)
Tvrdýite $Fe^{2+}Fe^{3+}_2Al_3(PO_4)_4(OH)_5 \cdot 6H_2O$	Tvr	*C2/c*	20.564	5.101	18.883	93.68	1976.7	(3)
Zincoberaunite $ZnFe^{3+}_5(PO_4)_4(OH)_5 \cdot 6H_2O$	Zbru	*C2/c*	20.837	5.162	19.250	93.252	2067.3	(4)

* (1) Vrtiška et al. (2022), (2) Tvrdý et al. (2022), (3) Sejkora et al. (2016), (4) Chukanov et al. (2017).

phase was referred to as *oxidized beraunite* and was later even curiously recognized under the old name *eleonorite* (Chukanov et al. 2017). The redefinition was based on the results of a detailed study of samples from the original 19th century discovery stored in the collections of TU Ber-

gakademie Freiberg (original Breithaupts specimen) and National Museum Prague (Fig. 7, 8).

Beraunite occurs in columnar and tabular crystals flattened on {100} and elongated along the *b* axis, often twinned on {100} (Fig. 9). The origin of beraunite has often been incorrectly sought in the oxidation of "green beraunite", i.e. current ferroberaunite. Indeed, brownish-red pseudomorphs of ferroberaunite do exist, especially in fibrous or needle-like form, and the changes from deep green to golden can be observed, for example, in samples from the Gravel Hill (Cornwall, England), Blaton (Belgium) or Folgosinho (Portugal) localities. However, a closer study of these oxidized phases has not yet been carried out and it is uncertain whether they are indeed beraunite. In contrast, the ruby-coloured transparent beraunite from iron-ore deposits clearly originate during direct crystallization.

From the Czech Republic, in addition to the type locality Hrbek, this mineral is known from other phosphate associations of sedimentary iron ores of the Barrandien area (Třenice, Krušná Hora; Černý et al. 2018) and the Krkonoše Piedmont Basin (Poniklá near Jilemnice; Škoda, Rus 2010; Vrtiška, Bednařík 2018), and it was also found in palaeorhyolite at Těškov near Rokycany (Janouš 1995; Lehrieder, Černý 1999). Transitional beraunite-ferroberaunite members are known from quartzites at the locality "Na Zoubku" near the village of Křeč in the Vysočina Region (also known as Černovice u Tábora; Vrtiška et al. 2017). Orange-yellow beraunite is reported by Čech, Staněk (1969) from phosphate accumulations in the Otov II pegmatite dyke near Poběžovice in the Plzeň Region. The characteristic accompanying minerals of beraunite are (natro)dufrénite and cacoxenite. The brownish radiating aggregates described from Krásno, Karlovy Vary Region, by Sejkora et al. (2006), can probably be considered as Fe^{3+} dominant beraunite.

Fig. 6 *Classification diagram for beraunite-related minerals with Fe^{3+} dominance at the M2–M4 sites based on the dominance in the M1 site. 1 beraunite – original specimen of Breithaupt, Hrbek (Vrtiška et al. 2022), 2 beraunite neotype, Hrbek (Vrtiška et al. 2022), 3 ferroberaunite holotype, Gravel Hill (Tvrdý et al. 2022), 4 zincoberaunite, Krásno (Tvrdý et al. 2020), 5 zincoberaunite cotype, Hagendorf South (Chukanov et al. 2016), 6 zincoberaunite holotype, Hagendorf South (Chukanov et al. 2016).*

Ferroberaunite

An investigation of the original material of beraunite proved the identity of this mineral with *eleonorite* (Vrtiška et al. 2022). The name *eleonorite* was discredited and the formula of beraunite $Fe^{3+}_6(PO_4)_4O(OH)_4 \cdot 6H_2O$ was adopted. To avoid duplicity of the mineral name "beraunite", the end-member with mixed iron valence was redefined and renamed to ferroberaunite (Tvrdý et al. 2022). From several studied specimens
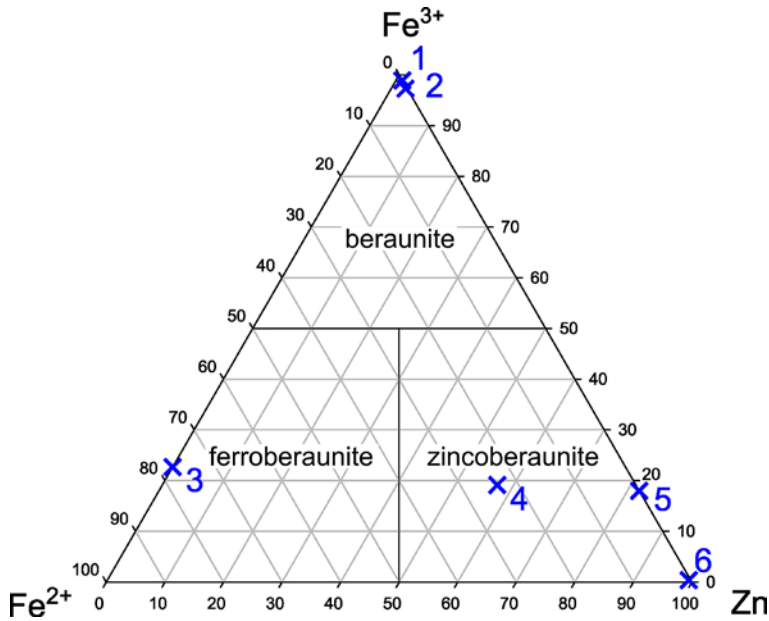

Fig. 7 *Orange red beraunite from the Hrbek mine, Czech Republic. FOV 0.5 mm across. Photo by L. Vrtiška.*

of the green-coloured "beraunites" (*e.g.* Blaton, Belgium; Svappavaara, Sweden; Hagendorf South, Germany; Krásno and Morašice, Czech Republic), a sample originating from the Gravel Hill mine, Perranzabuloe, Cornwall, England (United Kingdom) was chosen to define ferroberaunite (Fig. 10, 11). The reasons are excellent single-crystal X-ray data and the relative chemical purity, i.e., the absence of common isomorphic elements such as Al, Zn and Mn.

Dark green "beraunites" containing divalent iron described from a number of localities worldwide (Frondel 1949; Palache at al. 1951; van Tassel 1966; Moore 1970; Moore, Kampf 1992, and others) are consistent with ferroberaunite (Fig. 12).

In the Czech Republic, ferroberaunite is known from several localities. From the classic locality of the vanadium-rich wavellite "Na Zoubku" near Tábor, the mineralogical collection of the National Museum contains a specimen in which hemispherical radiating aggregates of beraunite-ferroberaunite of dark green to reddish--brown colour accompanied by cacoxenite and leucophosphite appear (Vrtiška et al. 2017).

In the Vysočina Region, another locality with the occurrence of ferroberaunite is situated in the abandoned pegmatite deposit Dolní Bory--Hatě. Beraunite from there consists of green and more rarely rusty reddish needles up to 2 mm in small cavities after altered and completely leached primary Fe-Mn-phosphate. Another form of occurrence is a thin dark green coating on cracks in quartz (Staněk 1997, 2009).

Dirty-green radial aggregates of a mineral corresponding to ferroberaunite were described by Korbel (1991) from the Huber open pit (Krásno deposit, Karlovy Vary Region). The mineral was identified by powder X-ray diffraction. The spectrally determined

Fig. 8 *Red beraunite crystals together with dark green spherical dufrénite from Hrbek, Czech Republic. FOV 11 mm across. Photo by L. Vrtiška.*
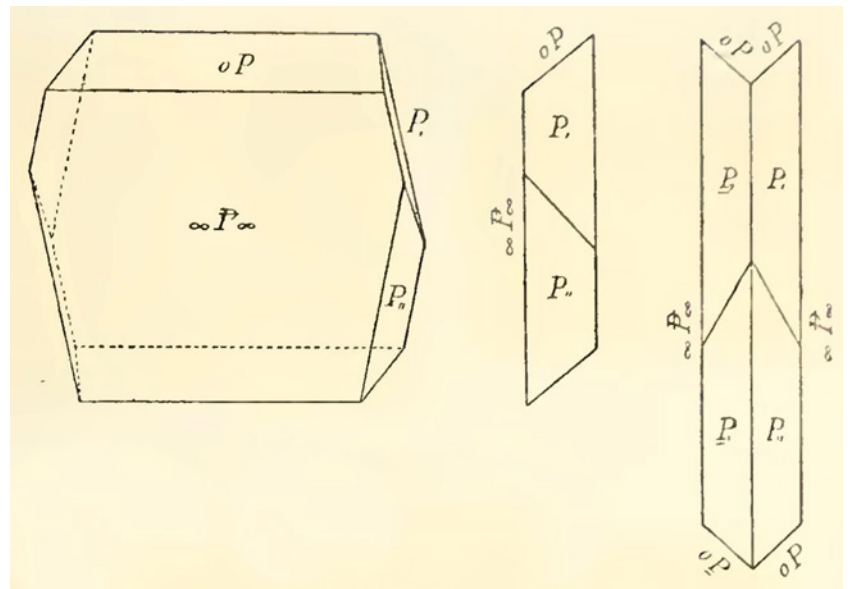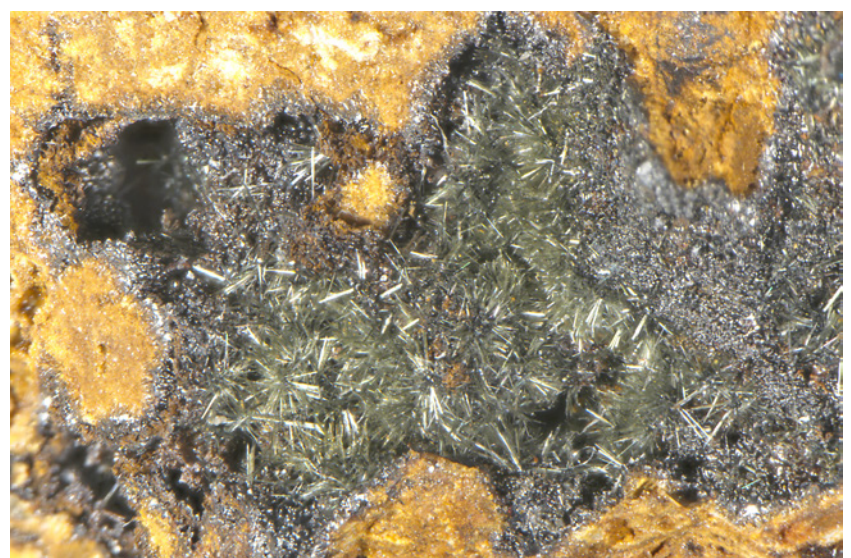

Fig. 9 *Crystal forms of beraunite (eleonorite) from the Rotläufchen mine, about 1.5 km north of Waldgirmes near Wetzlar in Hesse (Streng 1881).*

Fig. 10 *Ferroberaunite in olive-green acicular crystals on limonite matrix; holotype specimen. Gravel Hill, England. FOV 3 mm across. Photo by J. Tvrdý.*

Al and Zn contents were in the minority. Ferroberaunite with 0.30 *apfu* Zn and 0.76 *apfu* Al in green acicular crystals was identified by Tvrdý (2023; Fig. 13). Much higher zinc and aluminium contents were detected in beraunite-related mineral reported by Sejkora et al. (2006) in association with tvrdýite.

Zincoberaunite

Zincoberaunite, ideally $ZnFe^{3+}_5$ $(PO_4)_4(OH)_5 \cdot 6H_2O$, was described by Chukanov et al. (2016) as a new mineral on two specimens from the Hagendorf South pegmatite, Bavaria (Germany; Fig. 14). Accompanying phosphates are jungite, phosphophyllite and mitridatite, resp. flurlite, plimerite, schoonerite, phases of the parascholzite-scholzite series, robertsite, and altered phosphophyllite.

From the Czech Republic, zincoberaunite was newly identified on a sample of vein quartz from the Krásno deposit in the Karlovy Vary Region. The mineral forms thin needle-like crystals of yellow-grey to yellow-brown colours grouped in ray-like aggregates up to 2 mm (Tvrdý et al. 2020; Fig. 15).

Based on refined site occupancies and bond-valence considerations, the structural formula is $^{M1}(Zn_{0.81}Al_{0.19})$ $(OH)_2 {}^{M2}(Fe_{0.61}Al_{0.39})(OH)_2(H_2O)_2$ $^{M3}(Fe_{1.52}Al_{0.48})(H_2O)_2 {}^{M4}(Fe_{1.72}Al_{0.28})$ $(OH)(PO_4)_{3.83}(AsO_4)_{0.17}(H_2O)_2$. Electron-microprobe analyses support the obtained results. However, keeping the same cation occupancy at the $M2$-$M4$ sites, the ratio of Al^{3+} to Me^{2+} at the $M1$ site requires the presence of divalent cations as $(Zn_{0.57}Fe_{0.24}Al_{0.19})_{\Sigma1.00}$ $(Fe_{3.85}Al_{1.15})_{\Sigma5.00}[(PO_4)_{3.89}(AsO_4)_{0.10}$ $(SiO_4)_{0.01}]_{\Sigma4.00}[(OH)_{4.59}F_{0.24}O_{0.17}]_{\Sigma5.00}$ $(OH_2)_{4.00} \cdot 2H_2O$.
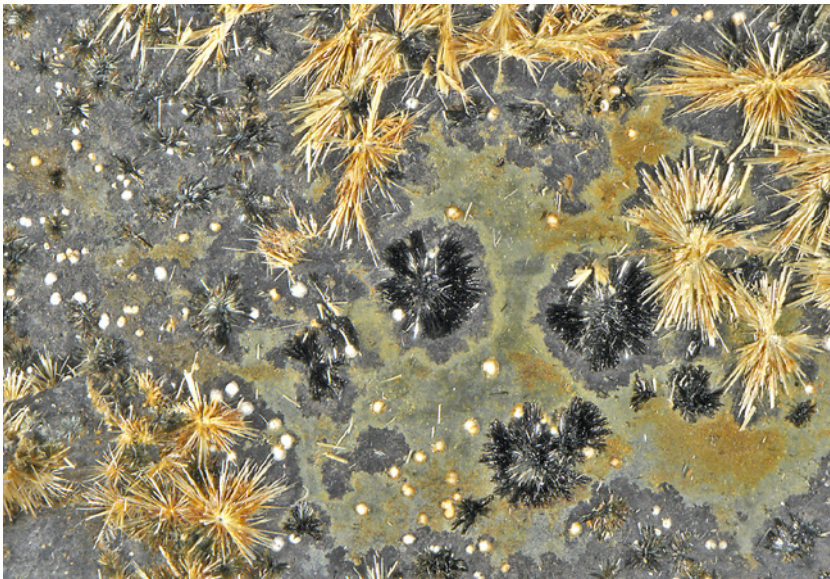

Fig. 11 *SEM image of a holotype ferroberaunite specimen from the Gravel Hill, England. Graphic scale. Photo by L. Vrtiška.*

Fig. 12 *Greenish-black radial ferroberaunite with beige ferristrunzite from Blaton, Belgium. FOV 10 mm across. Photo by J. Tvrdý.*
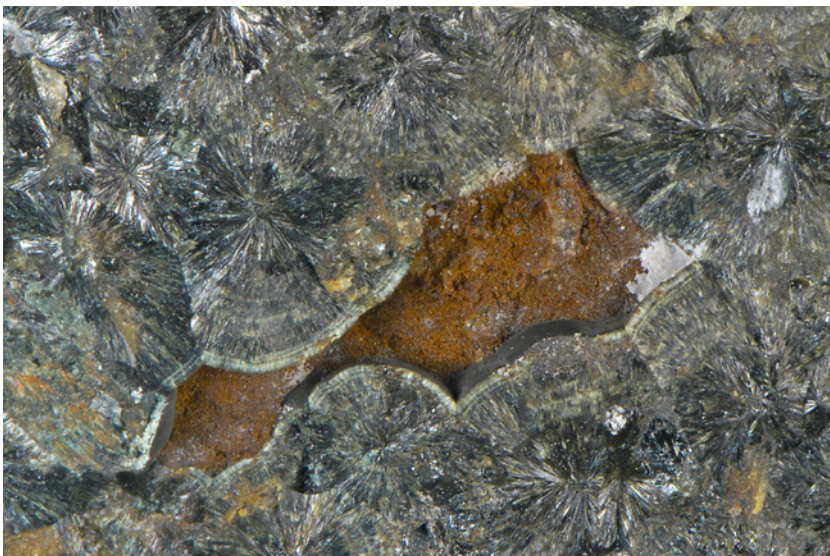
Fig. 13 *Ferroberaunite from Krásno, Czech Republic. FOV 8 mm across. Photo by L. Vrtiška.*

Individual prismatic zincoberaunite crystals exhibit a chemical zonation manifested by increasing Fe and decreasing Zn and Al contents from cores to rims. The mineral composition is close to the Zn-Al-rich members of the beraunite group known from the same locality (Sejkora et al. 2016; Fig. 16), but in this case, dominant occupancy of Zn at the *M*1 site was confirmed. Structure refinement revealed three different types of OH or H_2O, which play distinct role in structure bonding.

The importance of crystal chemical analysis is shown here, where the occupation of metals in individual *M*-sites must be determined. While zincoberaunite is Zn-dominated in the *M*1 site, in Zn-Al-rich (ferro)beraunite according to Sejkora et al. (2016) Zn is dispersed in all sites and does not dominate in any of them. Thus, a curious situation may appear when (ferro)beraunite contains more zinc than zincoberaunite (Fig. 17).

Manganese-rich beraunite

A Mn-bearing oxidized variety of beraunite with the empirical formula $Fe^{3+}_{5.65}Mn_{0.54}Na_{0.04}Ca_{0.03}Li_{0.01}(PO_4)_{4.06}(OH)_{5.95}(H_2O)_{4.81}$ was described from phosphate accumulations in granite at Mangualde in Portugal by Marzoni Fecia di Cossato et al. (1989). The nodules are composed of an intimate mixture of frondelite, mitridatite, beraunite and an amorphous phosphate. Other accompanying minerals are jahnsite-whiteite, strengite and pharmacosiderite. Manganese-rich beraunite forms needle-like crystals of a red colour. Optical properties, chemical composition, powder and single
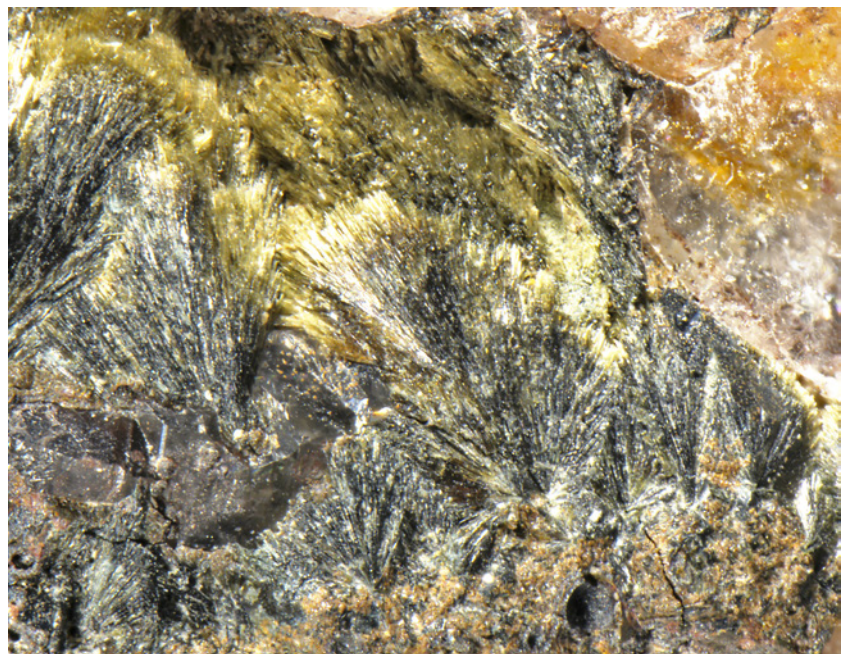

Fig. 14 *Spherical tufts of greenish grey-white zincoberaunite accompanied by fibres of a strunzite group mineral. Hagendorf South pegmatite, Germany. FOV 1.8 mm across. Photo by L. Vrtiška.*

Fig. 15 *Al-rich zincoberaunite from Krásno, Czech Republic. FOV 6 mm across. Photo by J. Tvrdý.*

Fig. 16 *Plot of total Fe vs. Al for zincoberaunite in comparison with data published for tvrdýite and Al-rich beraunite, all from the Huber open pit in Krásno (Tvrdý et al. 2020).*
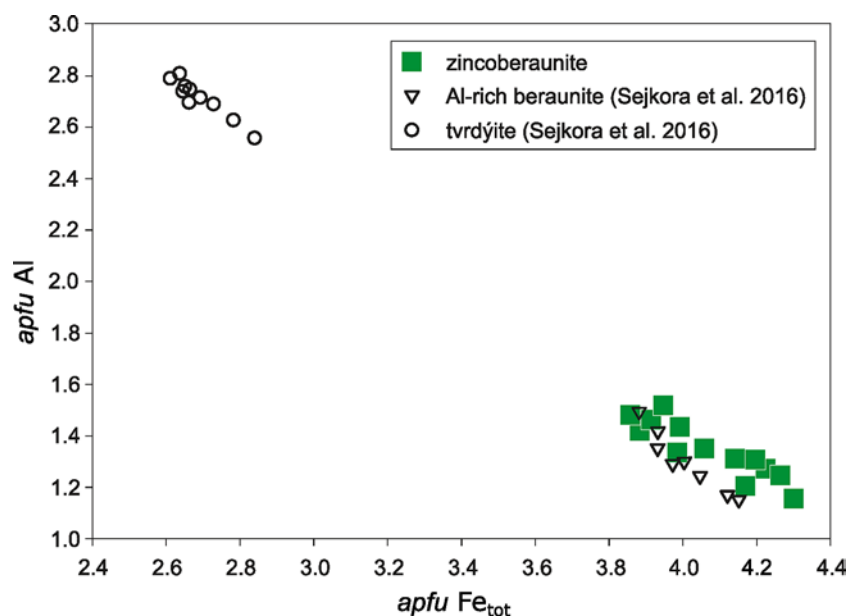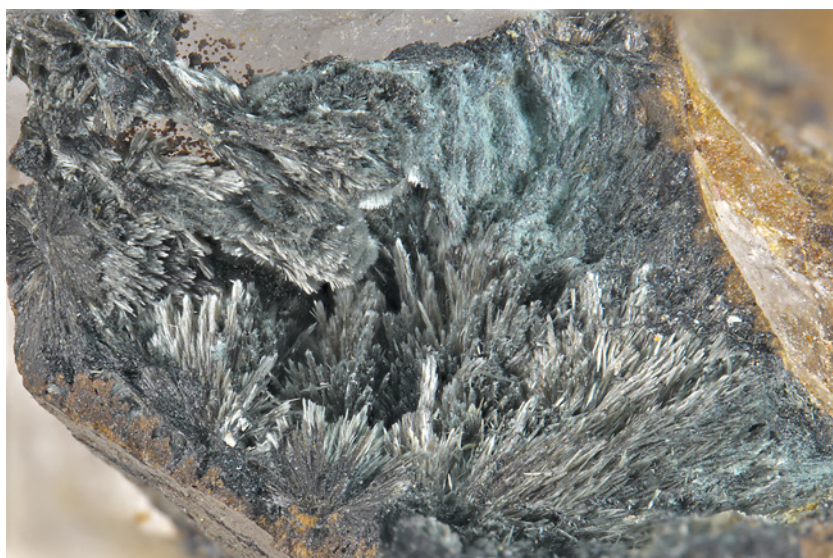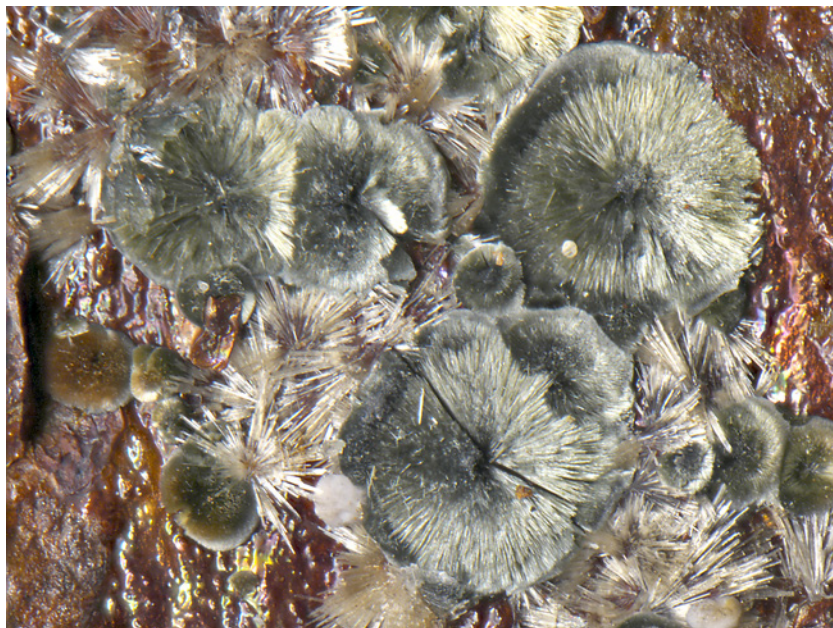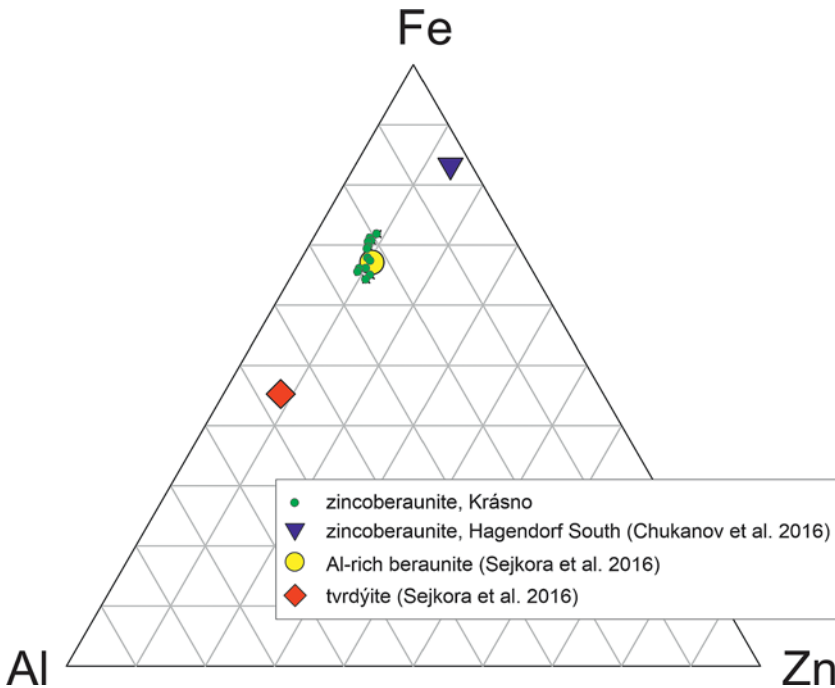
crystal X-ray data were determined. The structural analysis agrees with the data of Fanfani, Zanazzi (1967). Because of the predominance of Fe over Mn in the $M1$ site, the authors consider this mineral to be only a variety of beraunite.

Half a century later, manganese-rich beraunite (*Mn²⁺-bearing eleonorite*) was found in the Hagendorf South pegmatite in Bavaria (Aksenov et al. 2018). The mineral was characterized by single-crystal X-ray diffraction (SC-XRD), X-ray absorption near edge structure (XANES) and infrared spectroscopy (IR) methods. The empirical formula is $(Mn^{2+}_{0.58}Zn_{0.13}Mg_{0.04}Fe^{3+}_{5.24})_{\Sigma5.98}(PO_4)_4(H_2O,OH,O)_{11}$. However, since about half of the Mn occupies the $M1$ site and the rest is located on $M2$-$M4$ sites, it is not a separate mineral species either.

From the Czech Republic, a member of beraunite series (most probably ferroberaunite) with 0.36 - 0.70 (average 0.54) *apfu* Mn in the empirical formula was reported by Sejkora et al. (2006) in samples from phosphate accumulations found on the 5th level of the Huber mine at the Krásno deposit in the Karlovy Vary Region. Vrtiška et al. (2019a) described 0.12 - 0.21 *apfu* Mn in beraunite-ferroberaunite from oxidized manganese-iron ores at Morašice in the Pardubice Region (Fig. 18).

Fig. 17 *Comparison of zincoberaunite from Krásno with holotype zincoberaunite (from Hagendorf South) and related mineral phases from Krásno in the Al-Fe-Zn apfu ternary plot (Tvrdý et al. 2020).*

Fig. 18 *Grey (ferro)beraunite with elevated manganese content associated with whitish strunzite. Morašice, Czech Republic. FOV 3.5 mm across. Photo by L. Vrtiška.*

Fig 19. *Tvrdýite in clusters of long needle-like crystals; Krásno, Czech Republic. FOV 10 mm across. Photo by L. Vrtiška.*

Tvrdýite

Tvrdýite was described as a new mineral from the Sn-W-ore open pit at the Huber stock in the Krásno deposit (Karlovy Vary Region). It consists of fibrous crystals grouped in radial aggregates up to 3 mm large. It has a silvery to olive-greyish green colour and a pearly lustre (Fig. 19). It occurs in the cavity of vein quartz along with Al-rich beraunite, fluorapatite and pharmacosiderite (Sejkora et al. 2006, 2016).

From the Czech Republic, this mineral has also been identified in the collections of the National Museum Prague on a sample from the iron-ore deposit Krušná Hora near Beroun, Central Bohemia. It forms green to yellow-green radial concentric aggregates up to 4 mm in diameter, partly covered with jarosite (Fig. 20). The empirical formula is $(Fe^{2+}_{0.99}Mg_{0.01})_{1.00}$ $Fe^{3+}_{2.00}(Al_{2.18}Fe^{3+}_{0.68})_{2.86}(PO_4)_4(OH)_{4.57}$ $(OH_2)_4 \cdot 2H_2O$ (Vrtiška et al. 2019b; Vrtiška, Malíková 2020).

Furthermore, tvrdýite was found at the Hagendorf South locality in Germany (Weiß, Hochleitner 2017). From the same locality, Aksenov et al. (2018) marginally mentioned a transitional member of the tvrdýite-zincoberaunite series with 0.50 *apfu* Zn and 1.66 *apfu* Al in the empirical formula. This phase is already close to the hypothetical *zincotvrdýite* (Fig. 21).

Structurally related minerals

As mentioned above, the characteristic structural element of beraunite is the so-called *h*-cluster. In this sense, minerals of the dufrénite and rockbridgeite groups, of the gorma-
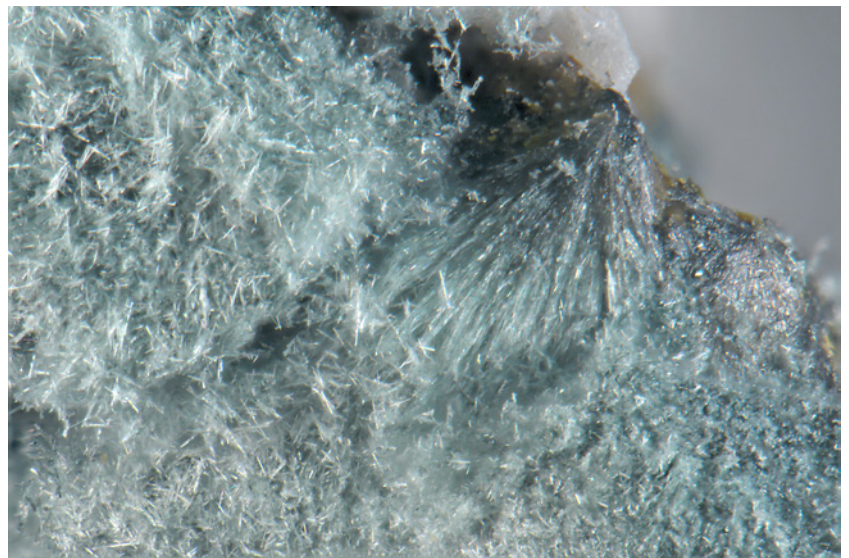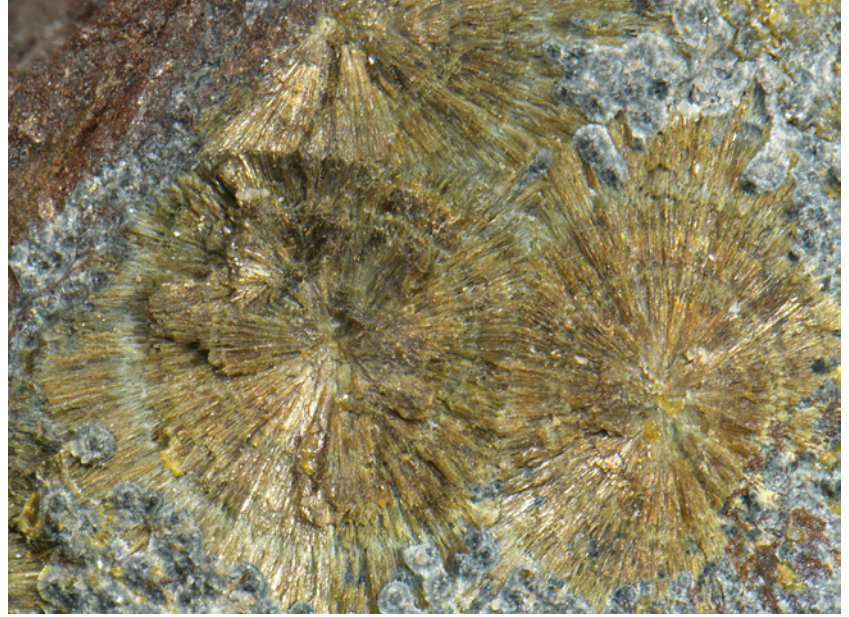

**Fig 20.** *Lustrous radial tvrdýite from Krušná Hora, Czech Republic. FOV 3 mm across. Photo L. Vrtiška.*

Fig 21. *Finely fibrous zincian tvrdýite from Hagendorf South (Germany). FOV 1.3 mm across. Photo L. Vrtiška.*

Fig. 22 *Crystal structure of dufrénite group minerals projected onto 010. Note the different numbering of M sites than in the beraunite group (data projection after Moore 1970).*
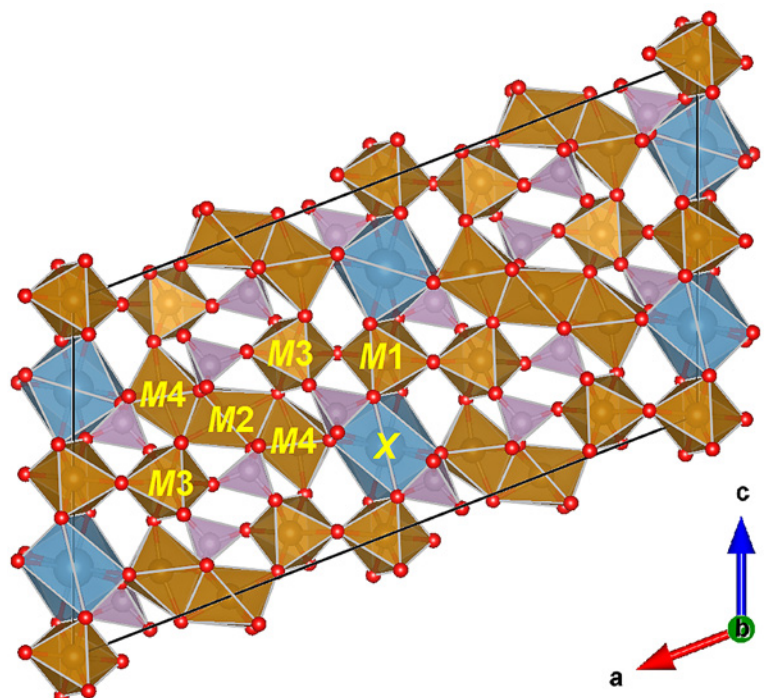
nite-souzalite series and lipscombite/barbosalite can be considered structurally related. In addition to divalent and trivalent Fe, which dominate in beraunite and ferroberaunite, individual structural sites may also be occupied by Al, Mn, Mg, Zn, Cu, and possibly other elements.

Minerals of the dufrénite group

The crystal structure of the dufrénite group minerals is very similar to that of beraunite. However, in channels parallel to the axis of elongation (i.e. the *b* axis), coordination polyhedra of Na, Ca in combination with vacancies are additionally integrated (Fig. 22). The central site in

the $M4 \equiv M2 \equiv M4$ trimer is assumed to be preferentially occupied by divalent cations (Fe^{2+}, Mn^{2+}, Mg; Table 5). This gives the structural formula $ABC_5(TO_4)_4(OH)_6 \cdot 2H_2O$, where *A* corresponds to the "channel" *X* site occupied by Ca, Na or vacancy, *B* to the *M*2 crystallographic site, which contain (but not only) all divalent cations, and *C* to the *M*1, *M*3 and *M*4 sites occupied by either Fe^{3+} or Al (Sejkora et al. 2007).

Six mineral species have been identified from the many possible combinations of elements (Table 6). Both aluminium-rich members of the group, burangaite and

Table 5 *Occupation of X and M structural sites in the dufrénite group minerals*

Mineral	*X*	*M*1	*M*2	*M*3	*M*4
Dufrénite	½Ca	Fe^{3+}	Fe^{2+}	$2Fe^{3+}$	$2Fe^{3+}$
Natrodufrénite*	Na	Fe^{3+}	Fe^{2+}	$2Fe^{3+}$	$2Fe^{3+}$
Gayite	Na	Fe^{3+}	Mn^{2+}	$2Fe^{3+}$	$2Fe^{3+}$
Bimbowrieite	Na	Fe^{3+}	Mg^{2+}	$2Fe^{3+}$	$2Fe^{3+}$
Burangaite	Na	Al^{3+}	Fe^{2+}	$2Al^{3+}$	$2Al^{3+}$
Matioliite	Na	Al^{3+}	Mg^{2+}	$2Al^{3+}$	$2Al^{3+}$

* According to CNMMN/CNMNC approved formula

Table 6 *Comparative data for minerals of the dufrénite group*

Mineral	Symbol	Space group	*a* (Å)	*b* (Å)	*c* (Å)	β (°)	V (Å³)	Ref.*
Dufrénite $Ca_{0.5}Fe^{2+}Fe^{3+}_5(PO_4)_4(OH)_6 \cdot 2H_2O$	Dfr	C2/c	25.84	5.126	13.78	111.20	1701.72	(1)
Natrodufrénite $NaFe^{2+}Fe^{3+}_5(PO_4)_4(OH)_6 \cdot 2H_2O$**	Ndf	C2/c	25.83	5.150	13.772	111.53	1704.19	(2)
Gayite $NaMn^{2+}Fe^{3+}_5(PO_4)_4(OH)_6 \cdot 2H_2O$	Gy	C2/c	25.975	5.177	13.929	111.29	1745.07	(3)
Bimbowrieite $NaMgFe^{3+}_5(PO_4)_4(OH)_6 \cdot 2H_2O$	Bbw	C2/c	25.995	5.151	13.892	111.61	1729.4	(4)
Burangaite $NaFe^{2+}Al_5(PO_4)_4(OH)_6 \cdot 2H_2O$	Brg	C2/c	25.099	5.049	13.438	110.88	1591.1	(5)
Matioliite $NaMgAl_5(PO_4)_4(OH)_6 \cdot 2H_2O$	Mti	C2/c	25.075	5.047	13.437	110.97	1587.9	(6)

* (1) Moore (1970), (2) Fontan et al. (1982), (3) Kampf et al. (2010), (4) Elliott, Kampf (2024), (5) Selway et al. (1997), Atencio et al. (2006). ** CNMMN/CNMNC approved formula.

Fig. 23 *Dark green kidney-shaped aggregates of natrodufrénite with a radial internal structure. Rochefort-en-Terre, Brittany, France (holotype specimen). FOV 25 mm across. Photo by L.-D. Bayle.*

matioliite, were reported from a few localities in the world. The Na-Mg-Fe-rich phase bimbowrieite is known only from the type locality of the White Rock feldspar mine in South Australia.

Gayite is reported from phosphate accumulations in the pegmatites of South America (Gigante pegmatite in the Córdoba Province, Argentina; Sapucaia mine, Minas Gerais, Brazil) and the Iberian Peninsula (Assunção Mine, Viseu, Portugal; Cañada pegmatite, Salamanca, Spain; Anthony et al. 2022). In the Czech Republic, it was found in the Cyrilov phosphate pegmatite (Vysočina Region; Škoda, Staněk 2010) and in the Sn--W-quartz-greisen deposit Krásno (Karlovy Vary Region; *Mn-rich dufrénite*, Sejkora et al. 2006).

Dufrénite and natrodufrénite are common minerals of secondary phosphate associations. They often occur together with beraunite in the same mineralisation environment as described in Chapter 2.2. Dark green dufrénite is a characteristic mineral of the classic locality Hrbek near Zaječov (Central Bohemian Region) as well as of the historic iron-ore deposits of the Lahn-Dill area in Hesse (Germany). An overview of localities associated with iron ores, sedimentary and metamorphic rocks in the Czech Republic was given by Vrtiška (2023).

Until the development of X-ray structural analysis in the 20th century, all green coloured hydrated basic phosphates were considered to be dufrénite (*kraurite*). Frondel (1949) regarded dufrénite to be a dimorph to beraunite with the same chemical formula. The crystal structure and valid chemical formula of dufrénite based on the analysis of Kinch, Butler (1886) were published by Moore (1970).

The most common mineral of this group is probably natrodufrénite. According to the results of a study of the original material found in 1861 in a small iron ore pit at Rochefort-en-Terre in Brittany, France (Fig. 23), Fe^{3+} rather than Fe^{2+} predominates at the $M2$ site. The results of Fontan et al. (1982) are therefore correct and the chemical formula given by IMA (Table 6) should be changed (Tvrdý 2023).

Minerals of the rockbridgeite group

Another group of minerals containing the *h*-cluster in the structural framework is the rockbridgeite group. However, there is a different occupation of octahedra in the central trimer $M2 \equiv M1 \equiv M2$, with trivalent iron in the centre and divalent cations at the sides (Fig. 24, Table 7). The structure-based formula is $A_2B_3(PO_4)_3(OH, H_2O)_5$, where A corresponds to the $M2$ site and contains all divalent cations and B includes the $M1$ and $M3$ sites do-
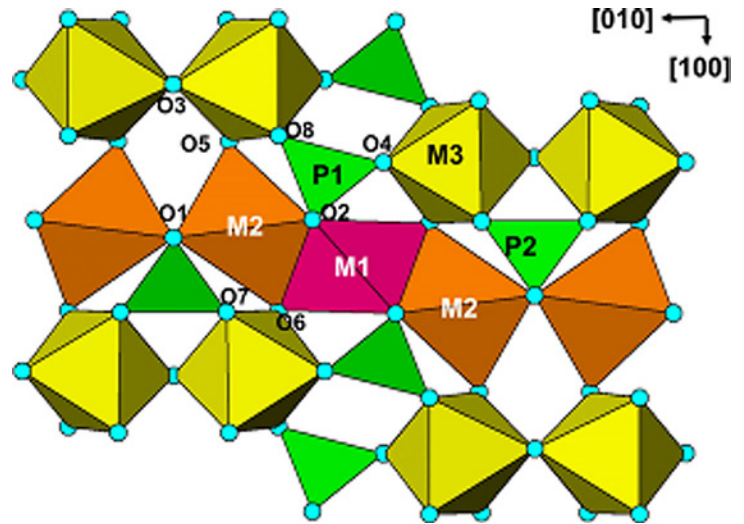

Fig 24 *Rockbridgeite structure projected along [001] (Grey et al. 2018). CC Attribution 4.0 License.*

Table 7 *Occupation of octahedral structural sites in rockbridgeite group minerals*

Mineral	$M1$	$M2$	$M3$
Rockbridgeite	Fe^{3+}	$2(Fe^{2+}_{0.5}Fe^{3+}_{0.5})$	$2Fe^{3+}$
Frondelite	Fe^{3+}	$2(Mn^{2+}_{0.5}Fe^{3+}_{0.5})$	$2Fe^{3+}$
Ferrorockbridgeite	Fe^{3+}	$2Fe^{2+}$	$2Fe^{3+}$
Ferrirockbridgeite	Fe^{3+}	$2(Fe^{3+}_{0.67}\square_{0.33})$	$2Fe^{3+}$
Manganrockbridgeite	Fe^{3+}	$2Mn^{2+}$	$2Fe^{3+}$
Plimerite	Fe^{3+}	$2Zn$	$2Fe^{3+}$

Table 8 *Ideal formulae and unit-cell parameters for rockbridgeite group minerals (Grey et al. 2019a)*

Mineral	Symbol	Space group	a (Å)	b (Å)	c (Å)	β (°)	V (Å³)	Ref.*
Rockbridgeite $(Fe^{2+}_{0.5}Fe^{3+}_{0.5})_2Fe^{3+}_3(PO_4)_3(OH)_5$	Rkb	*Bbmm*	13.783	16.805	5.172	–	1198.0	(1)
Frondelite $(Mn^{2+}_{0.5}Fe^{3+}_{0.5})_2Fe^{3+}_3(PO_4)_3(OH)_5$	Fnd	*Bbmm*	13.89	17.01	5.21	–	1231.0	(2)
Ferrorockbridgeite $Fe^{2+}_2Fe^{3+}_3(PO_4)_3(OH)_4(H_2O)$	Forck	*Bbmm*	14.008	16.808	5.190	–	1222.0	(3)
Ferrirockbridgeite $(Fe^{3+}_{0.67}\square_{0.33})_2Fe^{3+}_3(PO_4)_3(OH)_4(H_2O)$	Frck	*Bbmm*	13.853	16.928	5.192	–	1217.5	(4)
Manganrockbridgeite $Mn^{2+}_2Fe^{3+}_3(PO_4)_3(OH)_4(H_2O)$	Mrkb	P2$_1$/m	5.198	16.944	7.451	110.17	616.0	(5)
Plimerite $Zn_2Fe^{3+}_3(PO_4)_3(OH)_4(H_2O)$	Pme	*Bbmm*	13.865	16.798	5.151	–	1199.7	(6)

* (1) Moore (1970), (2) Lindberg (1949), (3) Grey et al. (2019a), (4) Grey et al. (2019b), (5) Grey et al. (2023), (6) Elliott et al. (2009).

minated usually by Fe^{3+} (Grey et al. 2019a). The charge balance caused by the presence of trivalent and divalent cations in this site is balanced by the substitution of OH for H_2O. The different group members are distinguished by the occupancy of the A (= $M2$) site (Table 8).

A triangular discrimination diagram with five fields was introduced for the Fe^{2+}, Mn^{2+} and Fe^{3+} dominated phases (Fig. 25). While rockbridgeite and frondelite are long known minerals (Frondel 1949; Lindberg 1949), ferrorockbridgeite, ferrirockbridgeite and manganrockbridgeite were defined in the context of this new classification scheme (Grey et al. 2019a, 2019b, 2023). Identification of individual species is complex and requires structural analysis and determination of the proportion of divalent and trivalent iron.

Minerals of the rockbridgeite group occur relatively frequently in *limonite* iron ore deposits and especially as a product of alteration of primary phosphates in granitic systems (Anthony et al. 2022). They are known from a large number of localities throughout the world. In the Czech Republic, rockbridgeite was identified in phosphate accumulations in pegmatites from Otov (Plzeň Region; Čech, Staněk 1969) and Dolní Bory (Vysočina Region; Staněk 1997, 2009), in peraluminous granite at Přibyslavice (Central Bohemian Region; Povondra et al. 1987),

in iron ores from Poniklá (Liberec Region; Škoda, Rus 2010), and in the Krásno Sn-W greisen deposit (Karlovy Vary Region; Sejkora et al. 2006). Plimerite is also known from Krásno (Sejkora et al. 2011).

Manganrockbridgeite has so far been reliably identified at two localities worldwide: from phosphate assemblages in Hagendorf-Süd, Bavaria, Germany (Grey et al. 2023) and from the Jocão claim, Conselheiro Pena County, Minas Gerais, Brazil (Tvrdý et al. 2024; Fig. 26). Both occurrences are very similar in terms of chemical composition, structural data and mineral association.

Gormanite-related minerals

According to Le Bail et al. (2003), the structure of souzalite-gormanite series consists of infinite chains of alternating FeO_6/MgO_6 and AlO_6 octahedra sharing faces and/or edges. These chains are connected by corners with clusters of three corner-sharing AlO_6 octahedra forming octahedral layers which are interconnected by PO_4 groups (Fig. 27). Similar to rockbridgeite, the $M^{2+} \equiv M^{3+} \equiv M^{2+}$ trimer is represented here in contrast to $M^{3+} \equiv M^{2+} \equiv M^{3+}$, which is much more frequent in mixed valence iron phosphate structures (Le Bail et al. 2003). Monoclinic kenngottite is structurally related (Table 9). The general formula for these phosphates can be expressed as $A_3B_4(PO_4)_4(OH)_6 \cdot H_2O$, where A contains divalent cations
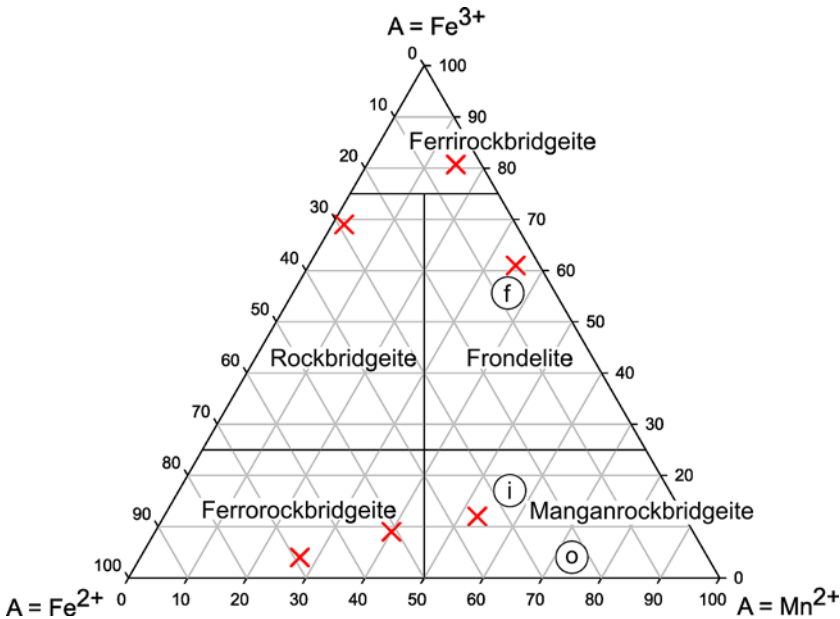

Fig. 25 *Classification diagram of the rockbridgeite group based on the occupation of the M2 site by Mn^{2+}, Fe^{2+} and Fe^{3+} (Grey et al. 2019). Plots of type specimens (two for ferrorockbridgeite) according to Grey et al. (2023) are marked with red crosses. Circles show mean values for the outer (o) and inner zone (i) of manganrockbridgeite as well as for frondelite (f) from the Jocão pegmatite (Tvrdý et al. 2024).*
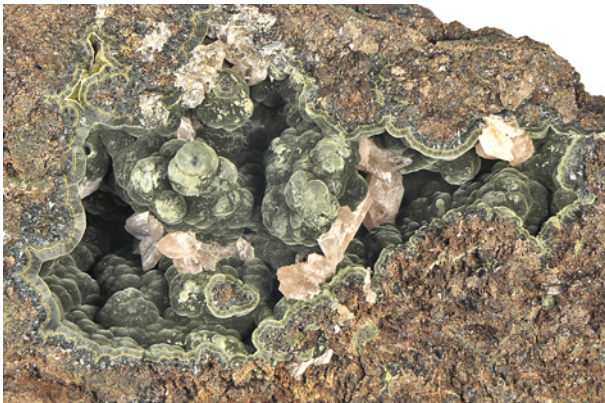

Fig. 26 *Cavity in brown correianevesite covered with a crust of green manganrockbridgeite and crystals of pale hureaulite. The outer and inner zones separated by a yellowish porous interlayer of kenngottite-like mineral are clearly distinct. Jocão claim, Minas Gerais (Brazil). FOV 23 mm (left) and 6 mm across (right). Photo by L. Vrtiška.*

(Mg, Fe^{2+}, Mn^{2+}) and *B* contains trivalent cations (Al, Fe^{3+}).

Minerals of this group are not abundant in phosphate associations. Souzalite is a rare hydrothermal alteration product of scorzalite in complex zoned granite pegmatites, in sedimentary phosphate nodules, and in high-pressure kyanite assemblages. Gormanite is reported from phosphate ironstones (Yukon Territory, Canada) and in fractures in tonalite (Bisbee, Arizona, USA; Anthony et al. 2022).

Kenngottite was formed by alteration of rockbridgeite group minerals in phosphate accumulations in quartz veins in greisen (Krásno, Czech Republic; Sejkora et al. 2019) and in pegmatites (Hagendorf South, Germany; Keck et al. 2022; probably also Jocão claim, Minas Gerais, Brazil; Tvrdý et al. 2024).

Lipscombite and barbosalite

The study of materials with Fe-P-OH-H complex structures is often motivated by their use in energy, catalysis and agriculture. Attention is also paid to the group of basic iron phosphates, which contain an octahedral face-sharing three-cluster and in most cases have a mixed iron valence (Sandineni et al. 2019; Poienar et al. 2020). So, for example, catalytic properties of synthetic barbosalite in oxidative dehydrogenation reactions was verified *e.g.* by Rouzies et al. (1995), and the ferric lipscombite-related phases were extensively studied as cathode for Li-ion batteries (Sandineni et al. 2019).

Basic structural data for both dimorph phases are given in Table 10, a projection of the layered structure is
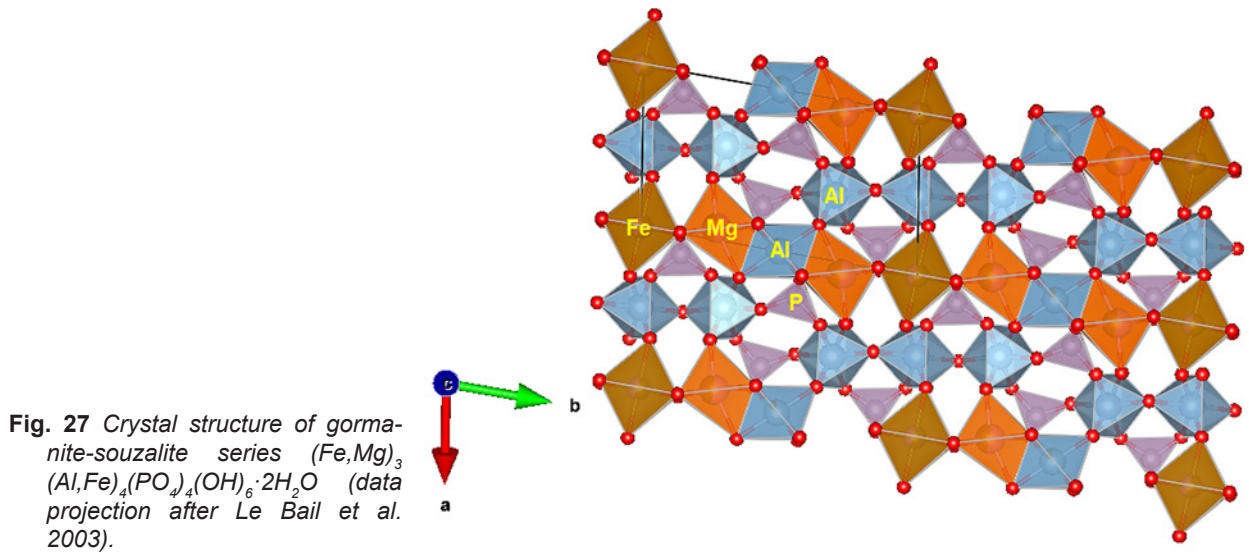
Fig. 27 *Crystal structure of gormanite-souzalite series $(Fe,Mg)_3 (Al,Fe)_4(PO_4)_4(OH)_6 \cdot 2H_2O$ (data projection after Le Bail et al. 2003).*

Table 9 *Comparative data for souzalite, gormanite and kenngottite*

Mineral	Symbol	Space group	*a* (Å)	*b* (Å)	*c* (Å)	α (°)	β (°)	γ (°)	*V* (Å³)	Ref.*
Gormanite $Fe^{2+}_3Al_4(PO_4)_4(OH)_6 \cdot 2H_2O$	Gm	*P*–1/*P*1	11.79	5.11	13.61	90.83	99.00	90.08	809.8	(1)
Souzalite $Mg_3Al_4(PO_4)_4(OH)_6 \cdot 2H_2O$	Sou	*P*–1	7.222	11.780	5.117	90.16	109.94	81.33	404.02	(2)
Kenngottite $Mn^{2+}_3Fe^{3+}_4(PO_4)_4(OH)_6 \cdot 2H_2O$	Kgt	*P*2/*a*	13.909	5.186	12.159	–	98.88	–	866.5	(3)

* (1) Sturman et al. (1981), (2) Le Bail et al. (2003), (3) Sejkora et al. (2019).

Table 10 *Comparative data for lipscombite and phosphates of the lazulite group**

Mineral	Symbol	Space group	*a* (Å)	*b* (Å)	*c* (Å)	β (°)	*V* (Å³)	Ref.**
Lipscombite $Fe^{2+}Fe^{3+}_2(PO_4)_2(OH)_2$	Lcb	*P*4₁2₁2	7.31	–	13.212	–	706.00	(1)
Barbosalite $Fe^{2+}Fe^{3+}_2(PO_4)_2(OH)_2$	Bbs	*P*2₁/c	7.25	7.46	7.49	120.25	349.94	(2)
Scorzalite $Fe^{2+}Al_2(PO_4)_2(OH)_2$	Scz	*P*2₁/c	7.15	7.31	7.25	120.58	326.23	(3)
Lazulite $MgAl_2(PO_4)_2(OH)_2$	Lzl	*P*2₁/c	7.144	7.278	7.228	120.5	323.81	(4)
Hentschelite $CuFe^{3+}_2(PO_4)_2(OH)_2$	Hsl	*P*2₁/*m*	6.984	7.786	7.266	117.68	349.89	(5)

* The lazulite group also includes arsenate wilhelmkleinite $ZnFe^{3+}_2(AsO_4)_2(OH)_2$ (Adiwidjaja et al. 2000). ** (1) Vencato et al. (1989), (2, 3) Lindberg, Christ (1959), (4) Giuseppetti, Tadini (1983), (5) Sieber et al. (1987).
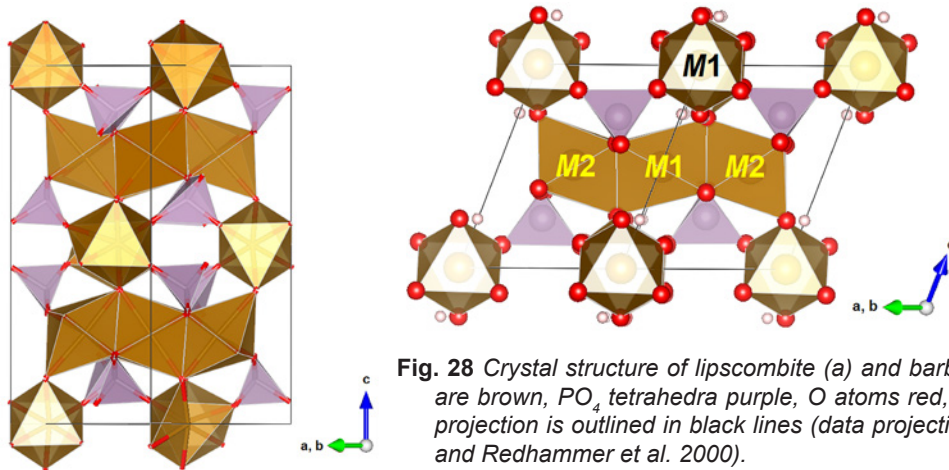
Fig. 28 *Crystal structure of lipscombite (a) and barbosalite (b). FeO_6 octahedra are brown, PO_4 tetrahedra purple, O atoms red, H atoms grey. The unit cell projection is outlined in black lines (data projection after Vencato et al. 1989 and Redhammer et al. 2000).*

shown in Fig. 28. According to Sandineni et al. (2019), the trimers $Fe^{3+} \equiv Fe^{2+} \equiv Fe^{3+}$ in lipscombite are face-shared to form the infinite chain of octahedra where Fe is partially occupied with ¾ Fe/octahedra in a 1:2 ratio of Fe^{2+} and Fe^{3+} in the chain. In barbosalite, a member of the lazulite group, instead of disordered face-shared chain, iron octahedra are ordered and they form isolated trimer of *h*-cluster.

Lipscombite and barbosalite are the most similar to beraunite in chemical composition. Its occurrences are associated with granitic pegmatites, where they were formed by oxidation and hydration of primary phosphates in the final stages of hydrothermal alteration. A number of localities are known throughout the world. In the Czech Republic, lipscombite is mentioned from Přibyslavice (Central Bohemian Region; Povondra et al. 1987), Otov (Plzeň Region; Čech, Staněk 1969) and in association with barbosalite from Cyrilov (Vysočina Region; Novák et al. 2000; Škoda et al. 2007).

Conclusions

Currently, the beraunite group contains four members with well-defined chemistry and structure. It is therefore ideal to study the influence of crystal chemistry on the physical properties and physicochemical environment of the formation of these minerals as well as minerals from related groups. The relatively simple chemical composition gives the impression that such study cannot be too difficult; however, the existence of four structural cation sites and two possible valence states of iron requires the use of very complex research methods. The frequent finely fibrous form and intergrowth of crystals usually makes sample separation for SC-XRD impossible, while the chemical zoning of crystals within a single aggregate complicates separation of a representative larger sample for some analyses (*e.g.* Mössbauer spectroscopy). Moreover, even a relatively small error in measurement of the Fe^{2+}/Fe^{3+} ratio can result in a large error in determination of the *M*1 site occupation. Thus, this mineral group remains a great challenge for mineralogists, crystallographers and geochemists.

References

ADIWIDJAJA G, FRIESE K, KLASKA KH, MOORE PB, SCHLUTER J (2000) The crystal structure of the new mineral wilhelmkleinite $ZnFe^{3+}_2(OH)_2(AsO_4)_2$. Z Kristallogr 215: 96-101

AKSENOV SM, CHUKANOV NV, GÖTTLICHER J, HOCHLEITNER R, ZARUBINA ES, RASTSVETAEVA RK (2018) Mn-bearing eleonorite from Hagendorf South pegmatite, Germany: Crystal structure and crystal-chemical relationships with other beraunite-type phosphates. Z Kristallogr 233: 2017-2099

ANTHONY JW, BIDEAUX RA, BLADH KW, NICHOLS MC, EDS (2022) Handbook of Mineralogy, Mineralogical Society of America, Chantilly, VA 20151-1110, USA. http://www.handbookofmineralogy.org/

ATENCIO D, COUTINHO JMV, MASCARENHAS YP, ELLENA JA (2006) Matioliite, the Mg-analogue of burangaite, from Gentil mine, Mendes Pimentel, Minas Gerais, Brazil, and other occurrences. Am Mineral 91: 1932-1936

BREITHAUPT A (1840) Beraunit, ein neues Glied der Phyllit-Ordnung. J Prakt Chem 20: 66-67 (in German)

BREITHAUPT A (1841) Beraunit. Vollständiges Handbuch der Mineralogie, Zweiter Band, I. Phyllites. Anhang 5: 156 (in German)

ČECH F, STANĚK J (1969) Minerály pegmatitů. In: BERNARD JH (ed.) Mineralogie Československa: 45-111. Academia Praha (in Czech)

ČERNÝ P, ČERNÝ P, VRTIŠKA L (2018) Fosfáty okolí Komárova a Hořovic. Minerál 26(5): 395-411 (in Czech)

CHUKANOV NV, PEKOV IV, GREY IE, PRICE JR, BRITVIN SN, KRZHIZHANOVSKAYA MG, KAMPF AR, DÜNKEL B, KECK E, BELAKOVSKIY DI, MACRAE CM (2016) Zincoberaunite, $ZnFe^{3+}_5(PO_4)_4(OH)_5 \cdot 6H_2O$, a new mineral from the Hagendorf South pegmatite, Germany. Mineral Petrol 111: 351-361

CHUKANOV NV, AKSENOV SM, RASTSVETAEVA RK, SCHÄFER C, PEKOV IV, BELAKOVSKIY DI, SCHOLZ R, DE OLIVEIRA LCA, BRITVIN SN (2017) Eleonorite, $Fe^{3+}_6(PO_4)_4O(OH)_4 \cdot 6H_2O$: validation as a mineral species and new data. Mineral Mag 81: 61-76

DUFRÉNOY A (1847) Traité de minéralogie. Tome 3. Victor Dalmont, Paris 1-685

ELLIOT P, KOLITSCH U, GIESTER G, LIBOWITZKY E, MC-CAMMON C, PRING A, BIRCH WD, BRUGGER J (2009) Description and crystal structure of a new mineral - plimerite, $ZnFe^{3+}_4(PO_4)_3(OH)_5$ - the Zn-analogue of rockbridgeite and frondelite, from Broken Hill, New South Wales, Australia. Mineral Mag 73: 131-148

ELLIOTT P, KAMPF AR (2024) Bimbowrieite, $NaMgFe^{3+}_5(PO_4)_4(OH)_6 \cdot 2H_2O$, a new dufrénite-group mineral from the White Rock No.2 quarry, South Australia, Australia. Mineral Mag 88(1): 90-96

FANFANI L, ZANAZZI P. F (1967) The crystal structure of beraunite. Acta Crystallogr 22: 173-181

FONTAN F, PILLARD F, PERMINGEAT F (1982) La natrodufrénite $(Na,\square)(Fe^{+++},Fe^{++})(Fe^{+++}, Al)_5(PO_4)_4(OH)_6 \cdot 2H_2O$, une nouvelle espèce minérale du groupe de la dufrénite. Bull Minéral 105: 321-326

FRONDEL C (1949) The dufrenite problem. Am Mineral 34: 513-540

GIUSEPPETTI G, TADINI C (1983) Lazulite, $(Mg,Fe)Al_2(OH)_2(PO_4)_2$: structure refinement and hydrogen bonding. N Jb Mineral, Mh 1983: 410-416

GREY IE, WILLIAMS T, KAMPF AR, CASHION JD, GOZUKARA Y, MACRAE CM, KECK E (2018) Non-stoichiometry and local order in minerals with the rockbridgeite structure. Eur J Mineral 30: 773-783

GREY IE, KAMPF AR, KECK E, CASHION JD, MACRAE CM, GOZUKARA Y, PETERSON VK, SHANKS FL (2019a) The rockbridgeite group approved and a new member, ferrorockbridgeite,$(Fe^{2+},Mn^{2+})_2(Fe^{3+})_3(PO_4)_3(OH)_4(H_2O)$, described from the Hagendorf Süd pegmatite, Oberpfalz, Bavaria. Eur J Mineral 31: 389-397

GREY I E, KAMPF AR, KECK E, CASHION JD, MACRAE CM, GOZUKARA Y, SHANKS FL (2019b) Ferrirockbridgeite, $(Fe^{3+}_{0.67}\square_{0.33})_2(Fe^{3+})_3(PO_4)_3(OH)_4(H_2O)$, and the oxidation mechanism for rockbridgeite-group minerals. Eur J Mineral 31: 585-594

GREY IE, HOCHLEITNER R, KAMPF AR, BOER S, MACRAE CM, CASHION JD, REWITZER C, MUMME WG (2023) Manganrockbridgeite, $Mn^{2+}_2Fe^{3+}(Fe^{3+})_3(PO_4)_3(OH)_4(H_2O)$, a new member of the rockbridgeite group, from the Hagendorf-Süd pegmatite, Oberpfalz, Bavaria. Eur J Mineral 35: 295-304

JANOUŠ F (1995) Minerály z Kněží hory u Těškova (okres Rokycany). Minerál 3(6): 367-369 (in Czech)

KAMPF AR, COLOMBO F, GONZÁLEZ DEL TÁNAGO J (2010) Gayite, a new dufrénite-group mineral from the Gigante granitic pegmatite, Córdoba province, Argentina. Am Mineral 95: 386-391

KECK E, GREY IE, MACRAE CM, BOER S, HOCHLEITNER R, REWITZER C, MUMME WG, GLENN AM, DAVIDSON C (2022) New secondary phosphate mineral occurrences and their crystal chemistry, at the Hagendorf Süd pegmatite, Bavaria. Eur J Mineral 34: 439-450

KINCH E, BUTLER FH (1886) On a new variety of mineral from Cornwall. Mineral Mag 7: 65-70

KORBEL P (1991) Supergene minerals from Horní Slavkov. Sbor Nár Muz (Praha), B47: 1-24

LE BAIL A, STEPHENS P. W, HUBERT F (2003) A crystal structure for the souzalite/gormanite series from synchrotron powder diffraction data. Eur J Mineral 15: 719-723

LEHRIEDER E, ČERNÝ P (1999) Der Steinbruch am Hügel Kněžský bei Těškov in Böhmen/Tschechien. Aufschluss 50: 79-85

LINDBERG ML (1949) Frondelite and the frondelite-rockbridgeite series. Am Mineral 34: 541-549

LINDBERG ML, CHRIST CL (1959) Crystal structures of the isostructural minerals lazulite, scorzalite and barbosalite. Acta Crystallogr 12: 695-697

MARZONI FECIA DI COSSATO Y, ORLANDI P, PASERO M (1989) Manganese-bearing beraunite from Mangualde, Portugal: mineral data and structure refinement. Can Mineral 27: 441-446

MOORE PB (1965) A structural classification of Fe-Mn orthophosphate hydrates. Am Mineral 50: 2052-2062

MOORE PB (1969) Basic ferric phosphates: A crystallochemical principle. Science 164: 1063-1064

MOORE PB (1970) Crystal chemistry of the basic iron phosphates. Am Mineral 55: 135-169

MOORE PB, KAMPF AR (1992) Beraunite: refinement, comparative crystal chemistry, and selected bond valences. Z Kristallogr 201: 263-281

NOVÁK M, SEJKORA J, COOPER MA (2000) Cyrilovite from Cyrilov, western Moravia, Czech Republic; new data on the type material. J Geosci 45: 101-106

PALACHE C, BERMAN H, FRONDEL C (1951) The System of Mineralogy of James Dwight Dana and Edward Salisbury Dana, Yale University 1837-1892, Volume II, 7th edition. John Wiley and Sons, Inc, New York.

POIENAR M, DAMAY F, ROUQUETTE J, RANIERI V, MALO S, MAIGNAN A, ELKAÏM E, HAINES J, MARTIN C (2020) Structural and magnetic characterization of barbosalite $Fe_3(PO_4)_2(OH)_2$. J Solid State Chem 287: 121357

POVONDRA P, PIVEC E, ČECH F, LANG M, NOVÁK F, PRACHAŘ I, ULRYCH J (1987) Přibyslavice peraluminous granite. Acta Univ Carol, Geol 1987/3: 183-283

REDHAMMER GJ, TIPPELT G, ROTH G, LOTTERMOSER W, AMTHAUER G (2000) Structure and Mössbauer spectroscopy of barbosalite $Fe^{2+}Fe^{3+}_2(PO_4)_2(OH)_2$, between 80 K and 300 K, Sample: T = 298 K. Phys Chem Miner 27: 419-429

ROUZIES D, MILLET JMM, SIEW HEW SAM D, VEDRINE JC (1995) Isobutyric acid oxidative dehydrogenation over iron hydroxyphosphates. I. Catalytic properties and role of water. Appl Catalysis A General 124: 189-203

SANDINENI P, GHOSH K, CHOUDHURY A (2019) Electrochemistry of illusive barbosalite, $Fe^{2+}Fe^{3+}_2(PO_4)_2(OH)_2$: An iron phosphate related to lipscombite structure. J Electrochem Soc 166: A3585-A3592

SEJKORA J, ŠKODA R, ONDRUŠ P, BERAN P, SÜSSER C (2006) Mineralogy of phosphate accumulations in the Huber stock, Krásno ore district, Slavkovský les area, Czech Republic. J Czech Geol Soc 1: 103-147

SEJKORA J, PLÁŠIL J, FILIP J (2011) Plimerite from Krásno near Horní Slavkov ore district, Czech Republic. J Geosci 56: 215-229

SEJKORA J, GREY IE, KAMPF AR, PRICE JR, ČEJKA J (2016) Tvrdýite, $Fe^{2+}Fe^{3+}_2Al_3(PO_4)_4(OH_2)_4\cdot2H_2O$, a new phosphate mineral from Krásno near Horní Slavkov, Czech Republic. Mineral Mag 80: 1077-1088

SEJKORA J, GREY IE, KAMPF AR (2019): Kenngottite, $Mn^{2+}_3Fe^{3+}_4(PO_4)_4(OH)_6(H_2O)_2$: a new phosphate mineral from Krásno near Horní Slavkov, Czech Republic. Eur J Mineral 31: 629-636

SELWAY JB, COOPER MA, HAWTHORNE FC (1997) Refinement of the crystal structure of burangaite. Can Mineral 35: 1515-1522

SHANNON RD (1976) Revised effective ionic radii and systematic studies of interatomic distances in halides and chalcogenides. Acta Crystallogr A64: 751-767

SIEBER NHW, TILLMANNS E, MEDENBACH O (1987) Hentschelite, $CuFe^{3+}_2(PO_4)_2(OH)_2$, a new member of the lazulite group, and reichenbachite, $Cu_5(PO_4)_2(OH)_4$, a polymorph of pseudomalachite, two new copper phosphate minerals from Reichenbach, Germany. Am Mineral 72: 404-408

ŠKODA R, RUS P (2010) Revize dufrenitu z Poniklé. Minerál 18(2): 119-123 (in Czech)

ŠKODA R, STANĚK J (2010) Gayite from granitic pegmatite at Cyrilov near Velké Meziříčí, Moldanubicum. Acta Mus Moraviae, Sci Geol: 95, 87-94

ŠKODA R, STANĚK J, ČOPJAKOVÁ R (2007) Mineral assemblages of the phosphate nodules from the granitic pegmatite at Cyrilov near Velké Meziříčí, Moldanubicum; part I - primary and exsolution phases. Acta Mus Moraviae, Sci Geol: 92, 59-74 (in Czech with English abstract)

STANĚK J (1997) Mineral assemblages of significant pegmatite dikes from the Hatě area near Dolní Bory, Western Moravia. Acta Mus Moraviae, Sci Nat 82: 3-19 (in Czech with English abstract)

STANĚK J (2009) Minerály Borů a Cyrilova u Velkého Meziříčí. Obec Bory, 1-102 (in Czech)

STEINMANN J (1826) Kákoxen. Archiv für die Gesamte Naturlehre 8: 446-446

STRENG A (1881) Ueber die Phosphate von Waldgirmes. N Jb Mineral Geolog Palaeontolog: 101-119

STURMAN BD, MANDARINO JA, MROSE ME, DUNN PJ (1981) Gormanite, $Fe^{2+}_3Al_4(PO_4)_4(OH)_6\cdot2H_2O$, the ferrous analogue of souzalite, and new data for souzalite. Can Mineral 19: 381-387

TVRDÝ J (2023) Revision of the beraunite group minerals and related phosphates. PhD Thesis. Masaryk University Brno. 1-124

TVRDÝ J, PLÁŠIL J, ŠKODA R (2020) New crystal-chemical data on zincoberaunite from Krásno near Horní Slavkov (Czech Republic). J Geosci 65(1): 45-57

TVRDÝ J, VRTIŠKA L, PLÁŠIL J, SEJKORA J, ŠKODA R, MASSANEK A, FILIP J, DOLNÍČEK Z, VESELOVSKÝ F (2021): The Beraunite problem. Acta Mineral Petrograph, Abstract Series 11: 47-47

TVRDÝ J, PLÁŠIL J, VRTIŠKA L, SEJKORA J, ŠKODA R, DOLNÍČEK Z, PETR M, VESELOVSKÝ F (2022) Ferroberaunite, $Fe^{2+}Fe^{3+}_5(PO_4)_4(OH)_5\cdot6H_2O$, a mixed-valence iron member of the beraunite series, from the Gravel Hill mine, Perranzabuloe, Cornwall, England. Mineral Mag 86: 363-372

TVRDÝ J, VRTIŠKA L, FILIP J, DOLNÍČEK Z, ŠKODA R, PETR M, MALÍKOVÁ R (2024) Manganrockbridgeite from the Jocão claim, Conselheiro Pena, Minas Gerais, Brazil: chemistry, spectroscopic and structural data. J Geosci 69: 87-98

VAN TASSEL R (1966) Mineraux secondaires phosphatés ferrifères (strunzite, beraunite, phosphosidérite, cacoxénite) de Blaton, Hainaut. Bull Soc Belge de Géol 75: 38-48

VELEBIL D, VRTIŠKA L, ČERNÝ P (2018) Důl Hrbek u Zaječova - slavné historické naleziště fosfátů. Minerál 26(5): 412-421 (in Czech)

VENCATO I, MATTIEVICH E, MASCARENHAS Y. P (1989) Crystal structure of synthetic lipscombite: A redetermination. Am Mineral 74: 456-460

VRTIŠKA L (2023) Naleziště sekundárních puklinových fosfátů v Českém masivu a jejich členění a porovnání v závislosti na typu hostitelské horniny. Bull Mineral Petrolog 31(2): 123-166 (in Czech with English abstract)

VRTIŠKA L, BEDNAŘÍK J (2018) Vivianit z Fe ložiska Poniklá u Jilemnice. Minerál 26(5): 452-454 (in Czech)

VRTIŠKA L, MALÍKOVÁ R (2020) New data on research of tvrdýite from Krušná hora near Beroun (Czech Republic). Bull Mineral Petrolog 28(2): 406-411 (in Czech with English abstract)

VRTIŠKA L, SEJKORA J, MALÍKOVÁ R, KADLEC T (2017) A revision and new findings of phosphates from the historical locality Černovice near Tábor (Czech Republic). Bull Mineral Petrolog 25(2): 277-305 (in Czech with English abstract)

VRTIŠKA L, TVRDÝ J, MALÍKOVÁ R, DOLNÍČEK Z (2019a) Manganese rich beraunite, strunzite and phosphosiderite from historical Fe-Mn ore deposit Morašice near Přelouč (Czech Republic). Bull Mineral Petrolog 27(2): 269-278 (in Czech with English abstract)

VRTIŠKA L, SEJKORA J, MALÍKOVÁ R (2019b) A study of secondary phosphates with allanpringite and tvrdýite from the abandoned iron deposit Krušná hora near Beroun (Czech Republic). Bull Mineral Petrolog 27(2): 231-246 (in Czech with English abstract)

VRTIŠKA L, TVRDÝ J, PLÁŠIL J, SEJKORA J, ŠKODA R, CHUKANOV NV, MASSANEK A, FILIP J, DOLNÍČEK Z, VESELOVSKÝ F (2022) Redefinition of beraunite, $Fe^{3+}_6(PO_4)_4O(OH)_4\cdot6H_2O$, and discreditation of the name eleonorite: a re-investigation of type material from the Hrbek Mine (Czech Republic). Eur J Mineral 34: 223-238

WEISS S, HOCHLEITNER R (2017) Neue Mineralien aus Hagendorf. Lapis 42(9): 42-46 (in German)

WŁODEK A, GROCHOWINA A, GOŁĘBIOWSKA B, PIECZKA A (2015) A phosphate-bearing pegmatite from Lutomia and its relationships to other pegmatites of the Góry Sowie Block, southwestern Poland. J Geosci 60: 45-72